MECHANIKA TEORETYCZNA
I STOSOWANA
Journal of Theoretical
and Applied Mechanics
4, 31, 1993

ON OPTIMAL PLASTIC DESIGN OF YOKE ELEMENTS

WŁADYSŁAW EGNER

ZDZISŁAWA KORDAS

MICHAŁ ŻYCZKOWSKI

Institute of Mechanics and Machine Design

Cracow University of Technology

The paper discusses optimal plastic design of yoke elements, like yokes, ends of connecting rods, chain links, etc. A design process consists of two steps: first, using the boundary perturbation method, we find a class of fully plastic solutions, and then choose the optimal one from among them. Unicriterial optimization may be employed if we look for maximal limit load-carrying capacity of constant-volume elements. However, if characteristic dimensions of the yoke are prescribed, then multicriterial optimization must be used. A comparison with some solutions obtained earlier by other authors is also given.

1. Introduction

As a yoke element we understand a hollow thick-walled load-carrying member mating with a transversal cylindrical bolt or pin (end of a connecting rod, bolt joint, chain link etc., Fig.1). The internal boundary is then assumed to be circular, whereas shape of the external boundary is free, subject to possible optimization. Circular shape of the external boundary, often used in practice, is not optimal from the viewpoint of material utilization, since the distribution of circumferential stresses in the "horizontal" cross-section (perpendicular to the axis of symmetry) is far from being uniform and a part of the material is not properly utilized.

In the present paper we discuss optimal plastic design of such elements. Similar problems were considered by Szczepiński (1966) (elements with optimal rectangular external contour), Szczepiński (1968), Szczepiński and Szlagowski (1990) (contour described by optimal broken line). They used statically admissible stress fields composed of piece-wise uniform stress distributions. Such an approach gives lower bound to the limit load-carrying capacity, or – for prescribed loading –

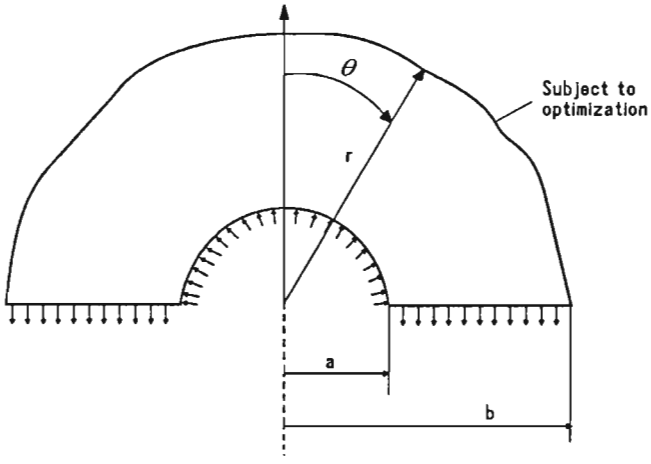

Fig. 1. A yoke element with external boundary subject to optimization

upper bound to the volume to be minimized. Zowczak (1989a,b) and (1989) improved this solution using geometrical approach, namely non-uniform stress fields constructed by the method of characteristics. However, no optimization problem was explicitly formulated and in his solutions some rigid zones remained.

Here we use an analytical approach based on the boundary perturbation method. Optimal design consists of two steps: first we look for a class of solutions showing full plastification at the stage of plastic collapse, and then choose the optimal one from among them.

Boundary perturbation method is now widely developed both in solid and in fluid mechanics (though not always under this name). Older results are presented in the monograph by Morse and Feshbach (1953), whereas a recent survey by Guz and Nemysh (1987) brings 310 references (mostly Ukrainian and Russian). The monograph by the same authors (1989) presents in detail two variants of this method. Recently, much attention to boundary perturbation method applied to elastic problems has been paid by Parnes (1987) and (1989). Fewer papers are devoted to boundary perturbation in the problems of plasticity; they were initiated by Ilyushin (1940), Ivlev (1957), and Spencer (1962). Applications of the boundary perturbation methods to optimal shape design are rather seldom; we mention here the paper by Schnack and Iancu (1989) who used numerically realized local perturbations.

A series of papers by Kordas and her collaborators, started in 1970 (cf Kordas and Życzkowski, 1970; Kordas and Skraba, 1977; Kordas, 1977 and 1979; Dollar and Kordas, 1980; Kordas and Postrach, 1990), used boundary perturbation method to the analysis of fully plastic states at the stage of collapse of perfectly plastic structural elements. This is the first step towards optimization (in most cases the

necessary condition), since the material in rigid or elastic zones at the stage of collapse is not properly utilized. In some cases this condition is not sufficient, and then additional optimization is necessary.

An example of such additional optimization is given in the paper by Bochenek, Kordas, and Życzkowski (1983), devoted to plastic optimization of doubly-connected cross-section of a bar under torsion with small bending. In the above problem just one boundary condition along each contour holds, thus it was always possible to find a class of solutions satisfying that condition and then to perform subsequent optimization.

In the present paper we apply a similar approach to plane problems where two boundary conditions along each contour must be satisfied and hence the existence of a broader class of fully plastic solutions is not obvious. It will be shown that such solutions do exist and may be subject to subsequent optimization. Depending on the formulation of the problem we arrive at unicriterial or multicriterial optimization. Both cases will be discussed in detail.

2. Assumptions, basic equations, boundary perturbation

We adopt the following assumptions:

• The material is perfectly plastic and incompressible, subject to either Huber-Mises-Hencky or Tresca yield condition.

• For relatively wide yoke elements plane strain state may be assumed. In cylindrical coordinates r, θ, z we assume $\varepsilon_z = 0$, then from the law of similarity of deviators we obtain $\sigma_z = \sigma_m$, the stress σ_z may be eliminated and the problem is statically pseudo-determinate: after this elimination two equilibrium equations and one yield condition determine three unknown stresses σ_r, σ_θ, $\tau_{r\theta}$. In this case both the above-mentioned yield conditions coincide, Życzkowski (1981), provided we employ the yield-point stress in shear τ_0 instead of the yield-point stress in tension σ_0

$$(\sigma_r - \sigma_\theta)^2 + 4\tau_{r\theta}^2 = 4\tau_0^2 \,. \tag{2.1}$$

In the case of the Tresca yield condition this form holds without the assumption of plane strain provided $\sigma_r \leq \sigma_z \leq \sigma_\theta$, but in the case under consideration this inequality is practically always satisfied. So, the case of plane stress belongs here as well.

• We consider a circular shape of the yoke element as the basic solution. Under the assumption of uniform radial loading along the inner contour $r = a$ and free outer contour $r = b$ we find the stress distribution in the fully plastic state

$$\sigma_r = 2\tau_0 \ln \frac{r}{b} \qquad \sigma_\theta = 2\tau_0\left(1 + \ln \frac{r}{b}\right) \qquad \tau_{r\theta} = 0 \,. \tag{2.2}$$

This solution is not optimal, since the resulting force transmitted by one half of the element

$$P = h \int_a^b \sigma_\theta dr = 2\tau_0 ah \ln \frac{b}{a} \tag{2.3}$$

where h denotes the transverse dimension of the element, may be raised. Indeed, the stresses σ_θ reach their upper bound $\sigma_\theta = 2\tau_0$ just for $r = b$, whereas inside the interval $a < r < b$ are smaller. They may increase as a result of an appropriate shape design. In what follows we admit $b = b(\theta)$, whereas we retain a = constant (the inner contacting element is usually circular).

To improve the above solution we use the boundary perturbation method. All the quantities under consideration, including the external contour $b = b(\theta)$, will be expanded into power series of a certain parameter α (to be specified later) of the type

$$\mathbf{X} = \sum_{i=0}^{\infty} \boldsymbol{X}_i \alpha^i \tag{2.4}$$

where

$$\mathbf{X} = \left[\sigma_r(r,\theta), \sigma_\theta(r,\theta), \tau_{r\theta}(r,\theta), b(\theta)\right]^\top. \tag{2.5}$$

The solution (2.2) and Eq (2.3) with $b(\theta) = b_0$ =constant will be regarded as the zeroth approximation. Equations of internal equilibrium are linear, hence for all terms of the series they retain their original form

$$\begin{aligned} &\frac{\partial \sigma_{r_i}}{\partial r} + \frac{1}{r}\frac{\partial \tau_{r\theta_i}}{\partial \theta} + \frac{\sigma_{r_i} - \sigma_{\theta_i}}{r} = 0 \\ &\frac{\partial \tau_{r\theta_i}}{\partial r} + \frac{1}{r}\frac{\partial \sigma_{\theta_i}}{\partial \theta} + 2\frac{\tau_{r\theta_i}}{r} = 0 \end{aligned} \tag{2.6}$$

whereas the non-linear yield condition (2.1) in view of $\tau_{r\theta_0} = 0$ is subject to linearization

$$\sigma_{r_i} - \sigma_{\theta_i} = f_i\left(\sigma_{r_0}, \sigma_{\theta_0}, ..., \sigma_{r_{i-1}}, \sigma_{\theta_{i-1}}, \tau_{r\theta_{i-1}}\right) \tag{2.7}$$

with $i = 1, 2, ...$ For the first two corrections we have

$$f_1 = 0 \qquad f_2 = \frac{1}{\tau_0}\tau_{r\theta_1}^2 . \tag{2.8}$$

Boundary conditions at the free boundary $b = b(\theta)$ with the normal n are

$$\begin{aligned} &\sigma_r \cos(\hat{n}r) + \tau_{r\theta} \cos(\hat{n}\theta) = 0 \\ &\tau_{r\theta} \cos(\hat{n}r) + \sigma_\theta \cos(\hat{n}\theta) = 0 \end{aligned} \tag{2.9}$$

and after expressing the cosines in terms of the function $b = b(\theta)$ (Kordas and Życzkowski, 1970), we obtain

$$\begin{aligned} b(\theta)\sigma_r - b'(\theta)\tau_{r\theta} &= 0 \\ b(\theta)\tau_{r\theta} - b'(\theta)\sigma_\theta &= 0 . \end{aligned} \tag{2.10}$$

Both these equations determine – in the case of full plastification – one function $b(\theta)$ as well as boundary values of stresses.

Expansion of Eq (2.10) into power series of α is more complicated, since the boundary itself is subject to perturbation. The increment of the independent variable Δr equals

$$\Delta r = \Delta b = \sum_{j=1}^{\infty} b_j(\theta)\alpha^j \tag{2.11}$$

and hence, replacing multiplication of series by a multiple series, we obtain

$$\begin{aligned} &\sum_{i=0}^{\infty}\sum_{k=0}^{\infty}\sum_{m=0}^{\infty} \alpha^{i+k} \frac{b_i(\theta)}{m!} \frac{\partial^m \sigma_{r_k}(r,\theta)}{\partial r^m}\Big|_{r=b_0} \Big[\sum_{j=1}^{\infty} b_j(\theta)\alpha^j\Big]^m = \\ &\sum_{i=0}^{\infty}\sum_{k=0}^{\infty}\sum_{m=0}^{\infty} \alpha^{i+k} \frac{b_i'(\theta)}{m!} \frac{\partial^m \tau_{r\theta_m}(r,\theta)}{\partial r^m}\Big|_{r=b_0} \Big[\sum_{j=1}^{\infty} b_j(\theta)\alpha^j\Big]^m \end{aligned} \tag{2.12}$$

and similarly for the second Eq (2.10). In the case under consideration, these expansions are essentially simplified, since $\tau_{r\theta_0} = b_0' = 0$.

At the inner contour $r = a$ the boundary conditions will not be specified. In any case, they are satisfied in integral form, it means that the "vertical" component of the resultant force acting on the pin or bolt is equal to $2P$, and the "horizontal" component vanishes. This is due to the equations of internal equilibrium (2.6), holding inside the body, and symmetry of solution assumed. A more precise formulation of the boundary conditions would require a solution of a rather complicated contact problem allowing for possible friction forces. This problem will not be considered. However, the resulting loadings will be calculated for particular solutions obtained and discussed from the point of view of their technical realization.

3. First-order perturbations

For $j = 1$ the Eqs (2.6) with the yield condition (2.7) and (2.8) resulting in $\sigma_{r_1} = \sigma_{\theta_1}$ may be reduced to one homogeneous hyperbolic equation

$$r^2 \frac{\partial^2 \tau_{r\theta_1}}{\partial r^2} - \frac{\partial^2 \tau_{r\theta_1}}{\partial \theta^2} + 3r \frac{\partial \tau_{r\theta_1}}{\partial r} = 0 . \tag{3.1}$$

After separation of variables we obtain the solution

$$\tau_{r\theta_1} = \frac{1}{r}\left[A_1 \sin\left(\sqrt{\lambda^2-1}\ln\frac{r}{b_0}\right) + B_1 \cos\left(\sqrt{\lambda^2-1}\ln\frac{r}{b_0}\right)\right]\sin\lambda\theta \tag{3.2}$$

where λ denotes the separation constant, in what follows regarded as a free parameter. A possible term with $\cos\lambda\theta$ was neglected in view of the coordinate system adopted (Fig.1), and symmetry required.

In order to present the formulae for subsequent perturbations in a more compact form we introduce the following simplified notations

$$\begin{aligned}
&\sin\left(\sqrt{\lambda^2-1}\ln\frac{r}{b_0}\right) = sl_r && \cos\left(\sqrt{\lambda^2-1}\ln\frac{r}{b_0}\right) = cl_r\\
&\sin\left(\sqrt{\lambda^2-1}\ln\frac{a}{b_0}\right) = sl_a && \cos\left(\sqrt{\lambda^2-1}\ln\frac{a}{b_0}\right) = cl_a\\
&\sin\left(2\sqrt{\lambda^2-1}\ln\frac{r}{b_0}\right) = sl_{2r} && \cos\left(2\sqrt{\lambda^2-1}\ln\frac{r}{b_0}\right) = cl_{2r}\\
&\sin\left(2\sqrt{\lambda^2-1}\ln\frac{a}{b_0}\right) = sl_{2a} && \cos\left(2\sqrt{\lambda^2-1}\ln\frac{a}{b_0}\right) = cl_{2a}
\end{aligned} \tag{3.3}$$

and rewrite Eq (3.2) briefly

$$\tau_{r\theta_1} = \frac{1}{r}\left(A_1 sl_r + B_1 cl_r\right)\sin\lambda\theta\,. \tag{3.4}$$

The relevant corrections for normal stresses are

$$\sigma_{r_1} = \sigma_{\theta_1} = \frac{1}{\lambda r}\left[\left(A_1 - \sqrt{\lambda^2-1}B_1\right)sl_r + \left(\sqrt{\lambda^2-1}A_1 + B_1\right)cl_r\right]\cos\lambda\theta + C_1 \tag{3.5}$$

where C_1 is an integration constant, regarded as an additional free parameter.

The boundary conditions for the first-order perturbations are found from Eq (2.12) by equating the coefficients of α at both sides. Substituting Eq (2.2) we obtain

$$\begin{aligned}
2\tau_0 b_1(\theta) &= -b_0\sigma_{r_1}\Big|_{r=b_0}\\
2\tau_0 b_1'(\theta) &= b_0\tau_{r\theta_1}\Big|_{r=b_0}
\end{aligned} \tag{3.6}$$

They determine unknown constants in Eqs (3.4) and (3.5), and, first of all, the function $b(\theta)$ corresponding to full plastification of the body. Since this function appears in both Eqs (3.6), a solution is possible if and only if

$$\tau_{r\theta_1} = -\frac{\partial\sigma_{r_1}}{\partial\theta}\Big|_{r=b_0} \tag{3.7}$$

Possibility of fulfilment of Eq (3.7) by Eqs (3.4) and (3.5) is not obvious. However, in the case under consideration it can be satisfied if $A_1\sqrt{\lambda^2-1}=0$, hence either $A_1 = 0$ or $\lambda = 1$. It is sufficient to put $A_1 = 0$. Indeed, if we substitute $\lambda = 1$, then all the terms with A_1 in Eqs (3.4) and (3.5) disappear, so the second alternative is reduced to the first one. Finally we obtain

$$\begin{aligned}
\tau_{r\theta_1} &= \frac{b_1}{r} cl_r \sin\lambda\theta \\
\sigma_{r_1} = \sigma_{\theta_1} &= \frac{B_1}{\lambda r}\left(-\sqrt{\lambda^2-1}\,sl_r + cl_r\right)\cos\lambda\theta + C_1 \qquad (3.8)\\
b_1(\theta) &= -\frac{B_1}{2\tau_0\lambda}\cos\lambda\theta - \frac{b_0}{2\tau_0}C_1 .
\end{aligned}$$

4. Second-order perturbations

For $j = 2$ Eqs (2.6) with the yield condition (2.7) may be reduced to one non-homogeneous hyperbolic equation

$$r^2\frac{\partial^2\tau_{r\theta_2}}{\partial r^2} - \frac{\partial^2\tau_{r\theta_2}}{\partial\theta^2} + 3r\frac{\partial\tau_{r\theta_2}}{\partial r} = -\frac{\lambda B_1^2}{2\tau_0 r^2}\left(1 + 2\sqrt{\lambda^2-1}\,sl_{2r} + cl_{2r}\right)\sin 2\lambda\theta . \quad (4.1)$$

The left-hand side of Eq (4.1) is identical to Eq (3.1), hence general solution of the homogeneous part will be written in the form (3.4) with the constants denoted by A_2 and B_2. A particular solution of the non-homogeneous equation (4.1) may be assumed proportional to $\sin 2\lambda\theta$ and finally we obtain

$$\tau_{r\theta_2} = \frac{1}{r}\left(A_2 sl_r + B_2 cl_r\right)\sin\lambda\theta - \frac{B_1^2}{8\tau_0\lambda r^2}\left[1 + \sqrt{\lambda^2-1}\,sl_{2r} + \left(2\lambda^2-1\right)cl_{2r}\right]\sin 2\lambda\theta. \quad (4.2)$$

Normal stresses may be found from Eqs (2.6), (2.7) and (2.8)

$$\begin{aligned}
\sigma_{r_2} &= \frac{1}{\lambda r}\left[\left(A_2 - \sqrt{\lambda^2-1}\,B_2\right)sl_r + \left(B_2 + \sqrt{\lambda^2-1}\,A_2\right)cl_r\right]\cos\lambda\theta + \\
&+ \frac{B_1^2}{8\tau_0\lambda^2 r^2}\left[-2\lambda^2 + \left(2\lambda^2-1\right)\sqrt{\lambda^2-1}\,sl_{2r} - \left(3\lambda^2-1\right)cl_{2r}\right]\cos 2\lambda\theta + \\
&+ \frac{B_1^2}{8\tau_0\lambda^2 r^2}\left[\lambda^2 - \sqrt{\lambda^2-1}\,sl_{2r} + cl_{2r}\right] + C_2 \qquad (4.3)\\
\sigma_{\theta_2} &= \frac{1}{\lambda r}\left[\left(A_2 - \sqrt{\lambda^2-1}\,B_2\right)sl_r + \left(B_2 + \sqrt{\lambda^2-1}\,A_2\right)cl_r\right]\cos\lambda\theta + \\
&+ \frac{B_1^2}{8\tau_0\lambda^2 r^2}\left[\left(2\lambda^2-1\right)\sqrt{\lambda^2-1}\,sl_{2r} - \left(\lambda^2-1\right)cl_{2r}\right]\cos 2\lambda\theta +
\end{aligned}$$

$$+ \frac{B_1^2}{8\tau_0\lambda^2 r^2}\left[-\lambda^2 - \sqrt{\lambda^2-1}\,sl_{2r} - \left(2\lambda^2-1\right)cl_{2r}\right] + C_2$$

where the constant C_2 is a new parameter.

The boundary conditions for the second-order perturbations, resulting from Eqs (2.10) and (2.12), are much more complicated. Formally, each expression on the left-hand side and on the right-hand side of Eq (2.12) contains seven terms with α^2. However, on the left-hand side of the first boundary condition one term vanishes (with σ_{r_0}), another two terms are subject to reduction in view of Eqs (3.6), and just four terms remain; on the right-hand side in view of $\tau_{r\theta_0} = b_0' = 0$ just one term does not vanish and making use of the zeroth approximation (2.2) we obtain

$$2\tau_0 b_2 + b_0\sigma_{r_2}\Big|_{r=b_0} + b_0 b_1 \frac{\partial\sigma_{r_1}}{\partial r}\Big|_{r=b_0} - \frac{\tau_0}{b_0}b_1^2 = b_1'\tau_{r\theta_1}\Big|_{r=b_0} \tag{4.4}$$

In the second boundary condition three non-zero terms remain on each side, but two terms are subject to reduction in view of Eqs (3.6) and we obtain

$$b_0 b_1 \frac{\partial\tau_{r\theta_1}}{\partial r}\Big|_{r=b_0} + b_0\tau_{r\theta_2}\Big|_{r=b_0} = 2\tau_0 b_2' + b_1'\sigma_{\theta_1}\Big|_{r=b_0} \tag{4.5}$$

Both these boundary conditions contain the unknown function $b_2 = b_2(\theta)$. It turns out that they may be satisfied simultaneously if

$$A_2 = -\frac{B_1 C_1}{2\tau_0}\sqrt{\lambda^2-1} \tag{4.6}$$

and for arbitrary B_2. In what follows, we put $B_2 = 0$. Indeed, leaving B_2 different from zero in (4.2) and (4.3), we repeat once more the first-order perturbation within the second-order perturbation (the functions governed by B_1 and B_2 are identical), and hence just the convergence of the series would get worse. Finally, the second-order perturbation of the boundary is given by

$$b_2(\theta) = -\frac{B_1^2}{16\tau_0^2 b_0} + \frac{b_0 C_1^2}{8\tau_0^2} - \frac{b_0 C_2}{2\tau_0} + \frac{B_1^2}{16\tau_0^2 b_0}\cos 2\lambda\theta\,.$$

5. The condition of constant volume

In view of the future optimization we evaluate the constants C_i from the condition of constant volume for a given ratio a/b_0. For an unperturbed circular shape this volume (of one half of the element shown in Fig.1) equals

$$V = \frac{\pi}{4}h\left(b_0^2 - a^2\right). \tag{5.1}$$

For a perturbed shape we have

$$V = \frac{h}{2}\int_0^{\frac{\pi}{2}} \left\{ \left[\sum_{i=0}^{\infty} b_i(\theta)\alpha^i \right]^2 - a^2 \right\} d\theta \tag{5.2}$$

and hence, to keep this volume independent of perturbations and equal to (5.1), we obtain the conditions

$$\begin{aligned} &\int_0^{\frac{\pi}{2}} b_1(\theta)d\theta = 0 \\ &\int_0^{\frac{\pi}{2}} \left[2b_0 b_2(\theta) + b_1^2(\theta) \right] d\theta = 0 \\ &\cdots\cdots\cdots\cdots \end{aligned} \tag{5.3}$$

They result in the following values of C_i

$$\begin{aligned} C_1 &= -\frac{2B_1}{\pi b_0 \lambda^2} \sin\frac{\lambda\pi}{2} \\ C_2 &= \frac{B_1^2}{8\pi\tau_0 b_0^2 \lambda^3} \left[-\left(\lambda^2 - 1\right)\lambda\pi + \left(\lambda^2 + 1\right)\sin\lambda\pi \right] \\ &\cdots\cdots\cdots\cdots \end{aligned} \tag{5.4}$$

hence

$$\begin{aligned} A_2 &= \frac{B^2\sqrt{\lambda^2 - 1}}{\pi\tau_0 b_0 \lambda^2} \sin\frac{\lambda\pi}{2} \\ b_1(\theta) &= \frac{B_1}{\pi\tau_0\lambda^2} \left(\sin\frac{\lambda\pi}{2} - \frac{\lambda\pi}{2}\cos\lambda\theta \right) \\ b_2(\theta) &= \frac{B_1^2}{16\pi^2\tau_0^2 b_0 \lambda^4} \left[\left(4 - \lambda^2\pi^2\right) - \lambda\pi\left(\lambda^2 + 1\right)\sin\lambda\pi - \right. \\ &\quad \left. -4\cos\lambda\pi + \lambda^4\pi^2\cos 2\lambda\theta \right] \\ &\cdots\cdots\cdots\cdots \end{aligned} \tag{5.5}$$

It is seen that the powers of the constant B_1 in all expressions are equal to the powers of the small parameter α. So, we introduce a new, dimensionless small parameter $\bar{\alpha}$ by the formula

$$\bar{\alpha} = \frac{B_1\alpha}{2\tau_0 b_0} \tag{5.6}$$

thus reducing the number of parameters by one. For example, the perturbed shape of the yoke element is now described by

$$\begin{aligned} b(\theta) &= b_0\Big\{1 + \Big(\frac{2}{\lambda^2\pi}\sin\frac{\lambda\pi}{2} - \frac{1}{\lambda}\cos\lambda\theta\Big)\bar{\alpha} + \Big[\Big(\frac{1}{\lambda^4\pi^2} - \frac{1}{4\lambda^2}\Big) - \\ &- \frac{1}{4\lambda^3\pi}\big(\lambda^2+1\big)\sin\lambda\pi - \frac{1}{\lambda^4\pi^2}\cos\lambda\pi + \frac{1}{4}\cos 2\lambda\theta\Big]\bar{\alpha}^2 + \ldots\Big\}. \end{aligned} \tag{5.7}$$

6. Transmitted force and reactive forces

The force transmitted by the cross-section $\theta = \pi/2$ (half of the total horizontal cross-section) is given by the integral generalizing (2.3), namely

$$P = h\int_a^{b(\frac{\pi}{2})}\sum_{i=0}^{\infty}\sigma_{0i}\Big(r,\frac{\pi}{2}\Big)\alpha^i\,dr\,. \tag{6.1}$$

where the upper limit of integration is given by the series (5.7) for $\theta = \pi/2$. Using consistently the small parameter $\bar{\alpha}$ and performing the operations on power series we write the final formula in the following dimensionless form

$$\begin{aligned} P^* &= \frac{P}{2\tau_0 b_0 h} = \frac{a}{b_0}\ln\frac{b_0}{a} + \Big(P_{10} + P_{11}\cos\frac{\lambda\pi}{2}\Big)\bar{\alpha} + \\ &+ \Big(P_{20} + P_{21}\cos\frac{\lambda\pi}{2} + P_{22}\cos\lambda\pi\Big)\bar{\alpha}^2 + \ldots \end{aligned} \tag{6.2}$$

where

$$\begin{aligned} P_{10} &= \frac{2a}{\lambda^2\pi b_0}\sin\frac{\lambda\pi}{2} \\ P_{11} &= -\frac{1}{\lambda\sqrt{\lambda^2-1}}sl_a - \frac{1}{\lambda}cl_a \\ P_{20} &= \Big(-\lambda^2 + \sqrt{\lambda^2-1}sl_{2a} - cl_{2a}\Big)\frac{b_0}{4\lambda^2 a} + \\ &\quad + \Big[\big(\lambda^2-1\big)\lambda\pi - \big(\lambda^2+1\big)\sin\lambda\pi\Big]\frac{a}{4\lambda^3\pi b_0} \\ P_{21} &= -\frac{2}{\lambda^3\pi}\sqrt{\lambda^2-1}\sin\frac{\lambda\pi}{2}sl_a + \frac{2}{\lambda^3\pi}\sin\frac{\lambda\pi}{2}cl_a \\ P_{22} &= \Big[\sqrt{\lambda^2-1}sl_{2a} + \big(\lambda^2-1\big)cl_{2a}\Big]\frac{b_0}{4\lambda^2 a}\,. \end{aligned} \tag{6.3}$$

The force (6.2) may be regarded as the limit load-carrying capacity of the element under consideration. More precisely, full plastification gives just a lower bound to the actual limit load-carrying capacity (an example of differences is given by Życzkowski (1981), pages 218 ÷ 221), but such differences are usually very small.

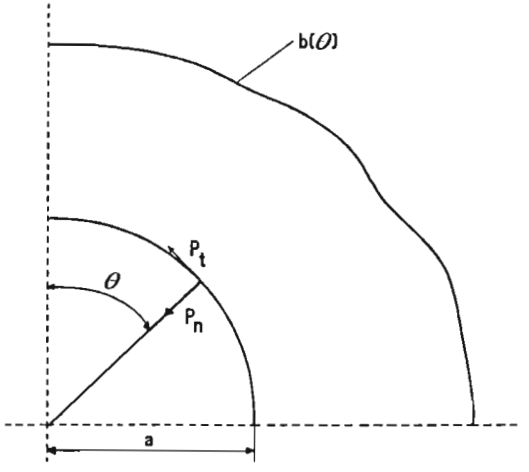

Fig. 2. Reactive forces at internal boundary $r = a$

The force P is equilibrated by the reactive force from the circular bolt with the radius a. This reactive force consists of two components (Fig.2), namely P_n resulting from normal surface tractions p_n and P_t from tangential surface tractions p_t

$$P_n = ah \int_0^{\frac{\pi}{2}} (-p_n) \cos\theta \, d\theta \qquad P_t = ah \int_0^{\frac{\pi}{2}} p_t \sin\theta \, d\theta \, . \tag{6.4}$$

To find the distribution of tractions $p_n(\theta)$ and $p_t(\theta)$ we should solve the problem of contact between the yoke and the bolt. This is a difficult problem and the results would essentially depend on mechanical properties of the bolt material and on the assumptions as regards friction between the surfaces in contact. We follow here an inverse procedure, namely assume the distribution of tractions resulting from the solution for the yoke obtained above

$$p_n = \sigma_r\Big|_{r=a} \qquad p_t = \tau_{r\theta}\Big|_{r=a} \tag{6.5}$$

and later discuss the perspectives of realization of such a distribution.

Making use of the solutions (2.2), (3.8), (4.2), and (4.3) we present the distribution of tractions at $r = a$ in the form

$$p_n = s_{00} + (s_{10} + s_{11}\cos\lambda\theta)\alpha + (s_{20} + s_{21}\cos\lambda\theta + s_{22}\cos 2\lambda\theta)\alpha^2 + \ldots$$
$$p_t = t_{11}\alpha\sin\lambda\theta + (t_{21}\sin\lambda\theta + t_{22}\sin 2\lambda\theta)\alpha^2 + \ldots \tag{6.6}$$

where s_{ij} and t_{ij} may be found from the above-mentioned solutions for $r = a$. Performing the integrations (6.4) we write final results in the dimensionless form

$$\begin{aligned} P_n^* &= \frac{P_n}{2\tau_0 b_0 h} = \frac{a}{b_0}\ln\frac{b_0}{a} + \Big(S_{10} + S_{11}\cos\frac{\lambda\pi}{2}\Big)\bar{\alpha} + \\ &+ \Big(S_{20} + S_{21}\cos\frac{\lambda\pi}{2} + S_{22}\cos\lambda\pi\Big)\bar{\alpha}^2 + \ldots \\ P_t^* &= \frac{P_t}{2\tau_0 b_0 h} = T_{11}\bar{\alpha}\cos\frac{\lambda\pi}{2} + \Big(T_{21}\cos\frac{\lambda\pi}{2} + T_{22}\cos\lambda\pi\Big)\bar{\alpha}^2 + \ldots \end{aligned} \tag{6.7}$$

where

$$\begin{aligned} S_{10} &= P_{10} \\ S_{20} &= P_{20} \\ S_{11} &= -\frac{1}{\lambda\sqrt{\lambda^2-1}}sl_a + \frac{1}{\lambda(\lambda^2-1)}cl_a \\ S_{21} &= \frac{2}{\lambda^3\pi\sqrt{\lambda^2-1}}\sin\frac{\lambda\pi}{2}sl_a + \frac{2}{\lambda^3\pi}\sin\frac{\lambda\pi}{2}cl_a \\ S_{22} &= \Big[-2\lambda^2 + \big(2\lambda^2-1\big)\sqrt{\lambda^2-1}sl_{2a} - \big(3\lambda^2-1\big)cl_{2a}\Big]\frac{b_0}{4\lambda^2(4\lambda^2-1)a} \\ T_{11} &= -\frac{\lambda}{\lambda^2-1}cl_a \\ T_{21} &= -\frac{2}{\lambda\pi\sqrt{\lambda^2-1}}\sin\frac{\lambda\pi}{2}sl_a \\ T_{22} &= \Big[1 + \sqrt{\lambda^2-1}sl_{2a} + \big(2\lambda^2-1\big)cl_{2a}\Big]\frac{b_0}{2(4\lambda^2-1)a}\,. \end{aligned} \tag{6.8}$$

It may be checked that $P_{ij} = S_{ij} + T_{ij}$ for any i, j, and hence the equilibrium is verified.

It should be noted that shearing stresses acting along the cross-section $\theta = \pi/2$ may also result in a transverse component of the loading, namely

$$Q = h\int_a^{b(\frac{\pi}{2})} \tau_{r\theta}\Big(r, \frac{\pi}{2}\Big)\,dr = h\int_a^{b(\frac{\pi}{2})} \sum_{i=0}^{\infty} \tau_{r\theta i}\Big(r, \frac{\pi}{2}\Big)\bar{\alpha}^i\,dr\,. \tag{6.9}$$

After integration one obtains

$$Q = -\bar{\alpha}\frac{1}{\sqrt{\lambda^2-1}}\sin\frac{\lambda\pi}{2}sl_a + \bar{\alpha}^2\Big\{\frac{4}{\pi\lambda^2}\sin\frac{\lambda\pi}{2}\Big(\sin\frac{\lambda\pi}{2} - \frac{\lambda\pi}{2}\cos\frac{\lambda\pi}{2}\Big) +$$
$$+ \sin\lambda\pi\Big[\frac{2}{\lambda\pi^2}\sin^2\frac{\lambda\pi}{2}\Big(cl_a - 1\Big) - \frac{1+\frac{a}{b_0}}{4\lambda\frac{a}{b_0}} - \frac{1}{4\lambda\frac{a}{b_0}(4\lambda^2-3)}\cdot \tag{6.10}$$
$$\cdot\ \Big((4\lambda^2-3)\Big(cl_{2a} - \frac{a}{b_0}\Big) - \sqrt{\lambda^2-1}(1+2\lambda^2)sl_{2a}\Big)\Big]\Big\}.$$

This component is of order one, and in comparison to P of order zero is small; moreover, for $\lambda = 2n$ (and this case will be discussed in detail) it vanishes, $Q = 0$, as it really takes place in most engineering applications. Hence the component Q will not be taken into account in subsequent optimization.

7. Unicriterial continuous optimization

Now we may formulate the optimization problems. The simplest statement looks as follows: from among the fully plastic solutions obtained above, we look for optimal λ and $\bar{\alpha}$, resulting in maximal limit carrying capacity P, Eq (6.2), under the constraint of constant volume V, Eq (5.2). Additional inequality constraints are imposed on the convergence of the power series used, Eq (2.4), and on the sign of the traction p_n at the contact surface, $r = a$, $0 \leq \theta \leq \pi/2$: it must be negative, since positive tractions (tensions) would not be transmitted. Another constraint is connected with transition from the yoke to the adjacent member, it means with the behaviour of the function $b(\theta)$ at $\theta = \pi/2$. Here we admit convex corner points, $b'(\pi/2) > 0$, but exclude concave corner points resulting in stress concentration. Then λ remains a continuous variable, but the above constraints must be checked for each solution obtained.

It turns out that the requirement imposed on convergence of the series is satisfied, with engineering accuracy, for $|\bar{\alpha}| \leq 0.25$; further, the design objective P is within the interval $-0.25 < \bar{\alpha} < 0.25$ a monotonic function of $\bar{\alpha}$ (with some unimportant exceptions), and hence it is sufficient to consider just boundaries of this interval, $\bar{\alpha} = 0.25$ and $\bar{\alpha} = -0.25$. The constraint $\sigma_r(a,\theta) \leq 0$ is then also satisfied. The approximation errors – with second-order perturbations taken into account – may be estimated as being of order $\bar{\alpha}^3 = 0.016$, it means 1.6 per cent. In view of the conditions (5.3) the volume is constant for any perturbed shape if a/b_0 is kept constant.

The dependence $P^* = f(\lambda)$ for various values of prescribed a/b_0 is shown in Fig.3 for $\bar{\alpha} = +0.25$, and in Fig.4 for $\bar{\alpha} = -0.25$. It may be seen that local maxima for $\bar{\alpha} = 0.25$ appear for λ close to 1, 4 and 8; for $\bar{\alpha} = -0.25$ for λ close to 2 and 6 (subsequent local maxima are lower).

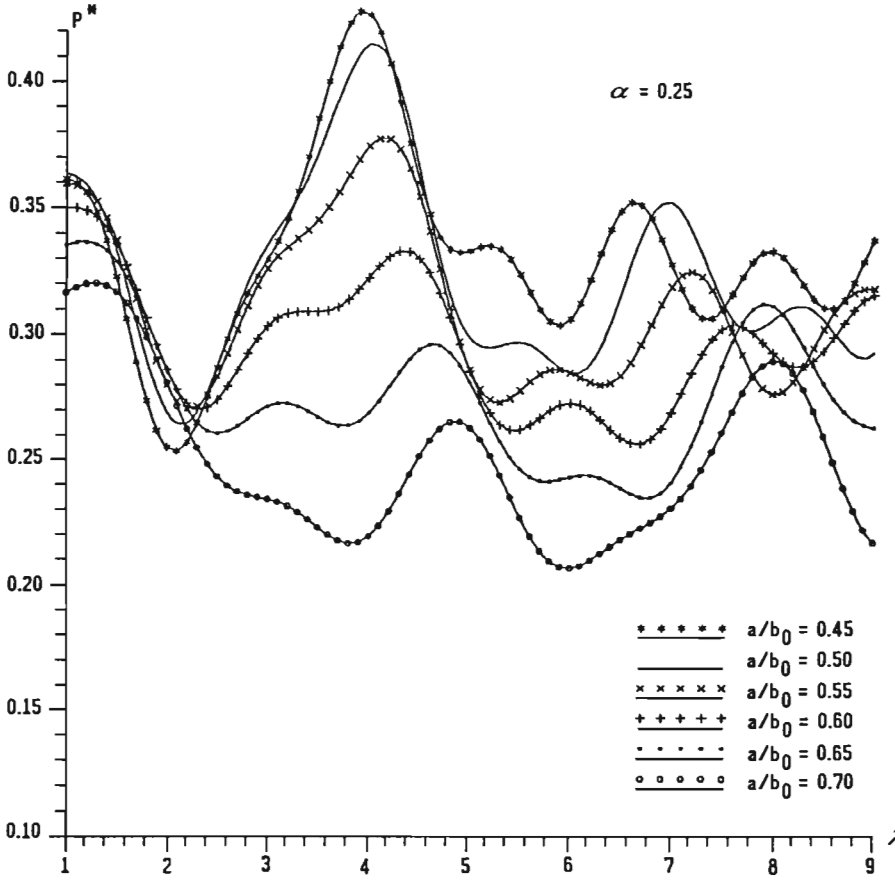

Fig. 3. Dependence of the force transmitted on the parameter λ for $\bar{\alpha} = 0.25$

The results are summarized in Fig.5, where all these maxima are compared to each other in terms of a/b_0, and the diagram $P_0^* = f(a/b_0)$ is also shown; P_0^* denotes here the limit carrying capacity for the unperturbed circular solution (2.3). If $a/b_0 < 0.57$, then the optimal solution is obtained for $\lambda \approx 4$, if $0.57 < a/b_0 < 0.63$ – for $\lambda \approx 6$, and if $a/b_0 > 0.63$ – for $\lambda \approx 1$. Local maxima for $\lambda \approx 2$ and $\lambda \approx 8$ are never the best. The geometric constraint $b'(\pi/2) \geq 0$ is always satisfied for $\lambda \approx 1$, and in the remaining cases it requires $\lambda_{opt} \geq 2$, $\lambda_{opt} \geq 4$,... etc. It is seen from Fig.3 and 4 that, as a rule, such conditions are satisfied; if not, then λ_{opt} should be replaced by the relevant even integer.

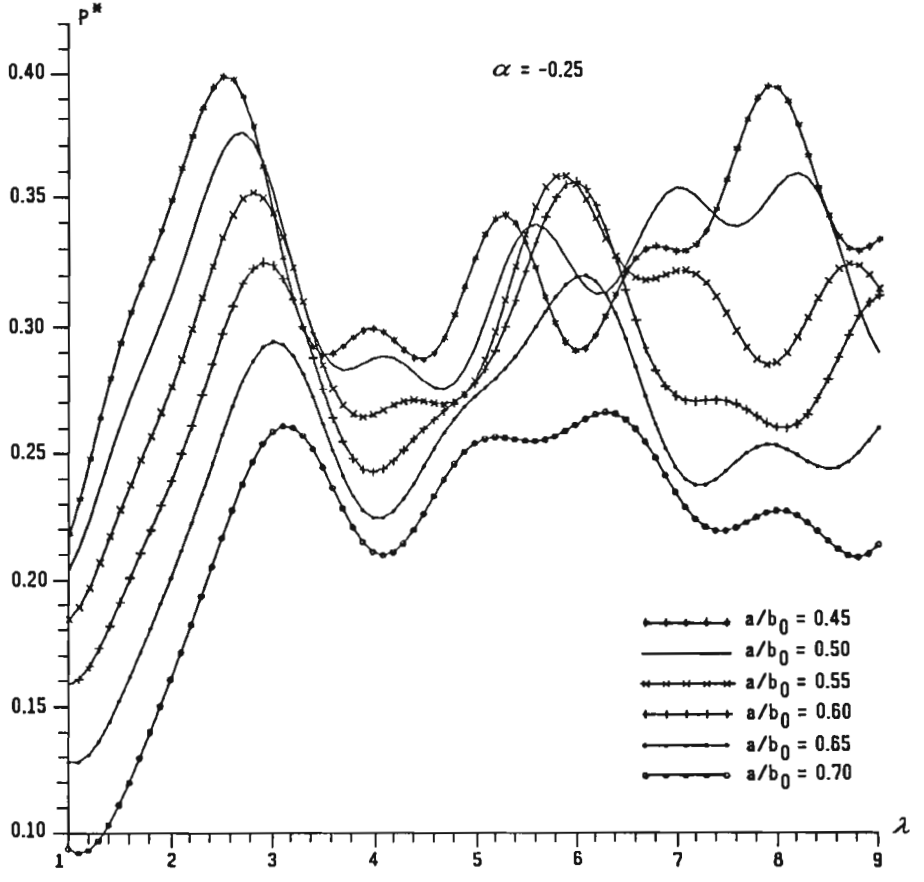

Fig. 4. Dependence of the force transmitted on the parameter λ for $\bar{\alpha} = -0.25$

Exemplary optimal shape and corresponding diagrams of circumferential stresses σ_θ (basic solution, subsequent perturbations and final sum up to the second perturbation) are shown in Fig.6 for $a/b_0 = 0.5$. We have then $\lambda_{opt} = 4.03$ for $\bar{\alpha} = +0.25$ and $P^* = 0.415$ compared to $P_0^* = 0.347$ for an unperturbed shape with the same volume. The profit on limit carrying capacity amounts here 19 per cent. In the case $a/b_0 = 0.6$ we have $\lambda_{opt} = 5.98$ for $\bar{\alpha} = -0.25$; to avoid the concave corner point we take $\lambda = 6$, then $b'(\pi/2) = 0$, $P^* = 0.358$ versus $P_0^* = 0.306$ and the profit amounts 17 per cent. The relevant shape for slightly different a/b_0, namely $a/b_0 = 0.584$, will be shown later in Fig.11. In the case $a/b_0 = 0.7$ we have $\lambda_{opt} = 1.20$ for $\bar{\alpha} = +0.25$ with $P^* = 0.320$ and relatively high profit 28 per cent, but this solution will be criticized below and the relevant shape is not shown.

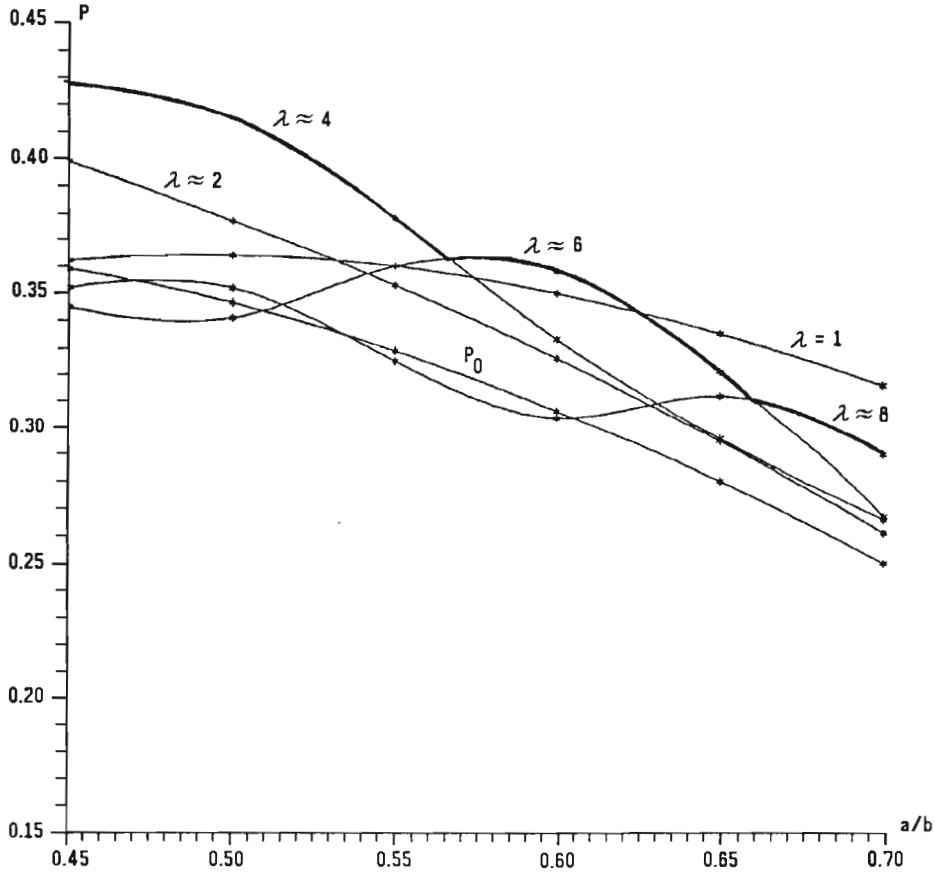

Fig. 5. Dependence of local optima on the ratio a/b_0

Now we have to discuss the distribution of reactive forces, resulting from the solutions obtained. The diagrams $P_n^* = f(a/b_0)$ and $P_t^* = f(a/b_0)$ obtained from (6.7) for λ giving local maxima of P^* are shown in Fig.7. It is seen that for λ close to even integers most of the force P^* is transmitted by normal reaction P_n^*, the share of P_t^* is small and usually such a reaction may be realized as a result of friction forces. In the case $\lambda \approx 1$ the situation is quite different: both components of the reactive force, P_n^* and P_t^*, are almost equal to each other, such magnitude of P_t^* very seldom can be realized in engineering applications, and this solution should rather be left out of consideration. So, $\lambda \approx 6$ hould be regarded as optimal up to $a/b_0 = 0.66$, and for $a/b_0 > 0.66$ the optimal solutions with $\lambda \approx 8$ are recommended.

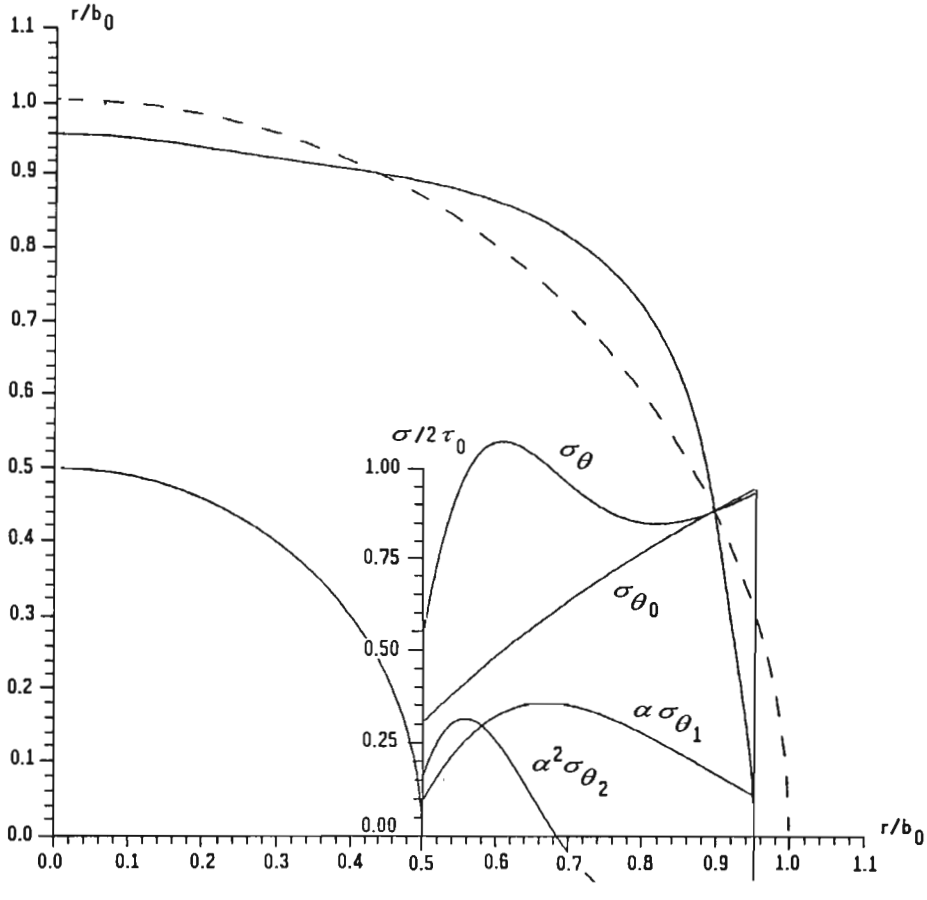

Fig. 6. Optimal shape for $a/b_0 = 0.5$ (unicriterial optimization) and relevant circumferential stresses

Fig.8 shows such a shape for $a/b_0 = 0.7$, $\bar{\alpha} = +0.25$, $\lambda_{opt} = 8.02$, $P^* = 0.290$ versus $P_0^* = 0.250$, hence the profit equals here 16 per cent. The share of tangential reaction is rather small here ($P_t^* = 0.049$), and may be considered as realistic.

If the friction at the surface of contact is absent, we might formulate another optimization problem: look for optimal λ and $\bar{\alpha}$, resulting in maximal normal reactive force P_n^*, Eq (6.7), under the constraint of constant volume and the remaining constraints as before. We give here the solution for such a formulation, though it will be concluded with some critical remarks.

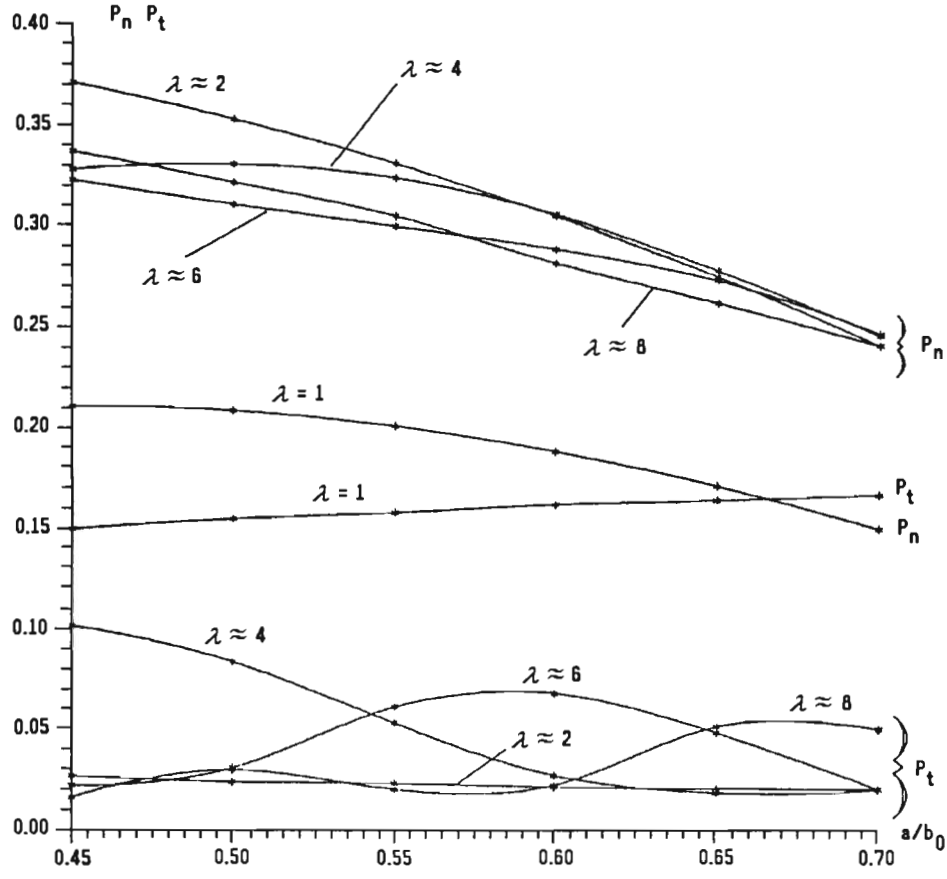

Fig. 7. Dependence of normal and tangential reactive forces on the ratio a/b_0 for local optima

The dependence $P_n^* = f(\lambda)$ for various values of prescribed a/b_0 is shown in Fig.9 for $\bar{\alpha} = -0.25$; the maxima for $\bar{\alpha} = +0.25$ are lower and are not quoted. Upper bounds of P_n^* are obtained for $\lambda = 1$ (this singular case may be determined by the formulae derived, if an additional limiting procedure is employed). However, for $\bar{\alpha} = -0.25$ the interval $1 \leq \lambda < 2$ must be excluded, since then $b'(\pi/2) < 0$ and a concave corner point at the contour would appear. So, $\lambda_{opt} = 2$ for any a/b_0 in this formulation.

An exemplary optimal shape for $a/b_0 = 0.6$ is shown in Fig.10 with the relevant circumferential stress distribution. The design objective equals $P_n^* = 0.352$ compared to $P_0^* = 0.306$ for an unperturbed shape. However, this solution should be criticized from the engineering point of view: the tangential component of the reactive force, P_t^*, is here negative with a substantial value ($P_t^* = -0.113$), it means in the sense opposite to usual friction forces, and probably cannot be

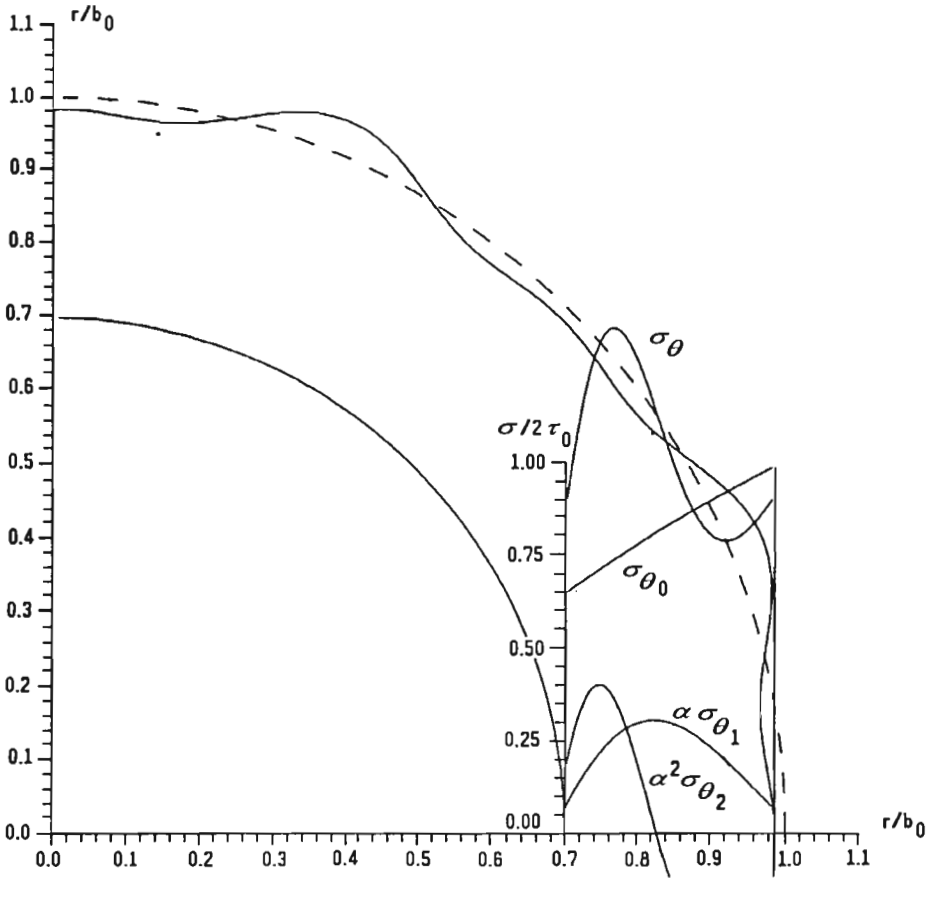

Fig. 8. Optimal shape for $a/b_0 = 0.7$ (unicriterial optimization) and relevant circumferential stresses

realized. Practically, if friction forces are absent, for the value $a/b_0 = 0.6$ the solution for $\lambda \approx 4$ gives the optimal shape, namely it maximizes P^* with almost vanishing P_t^*.

8. Unicriterial integer optimization

In many engineering applications of yoke elements the constraint connected with transition to the adjacent member is formulated in a stronger form then that discussed in Sec.7. Namely, even convex corner points are excluded, the tangent at $\theta = \pi/2$ is assumed to be vertical, it means $b'(\pi/2) = 0$. In view of Eq (5.7) we have then $\lambda = 2n$, where n is an arbitrary integer. We arrive here at an

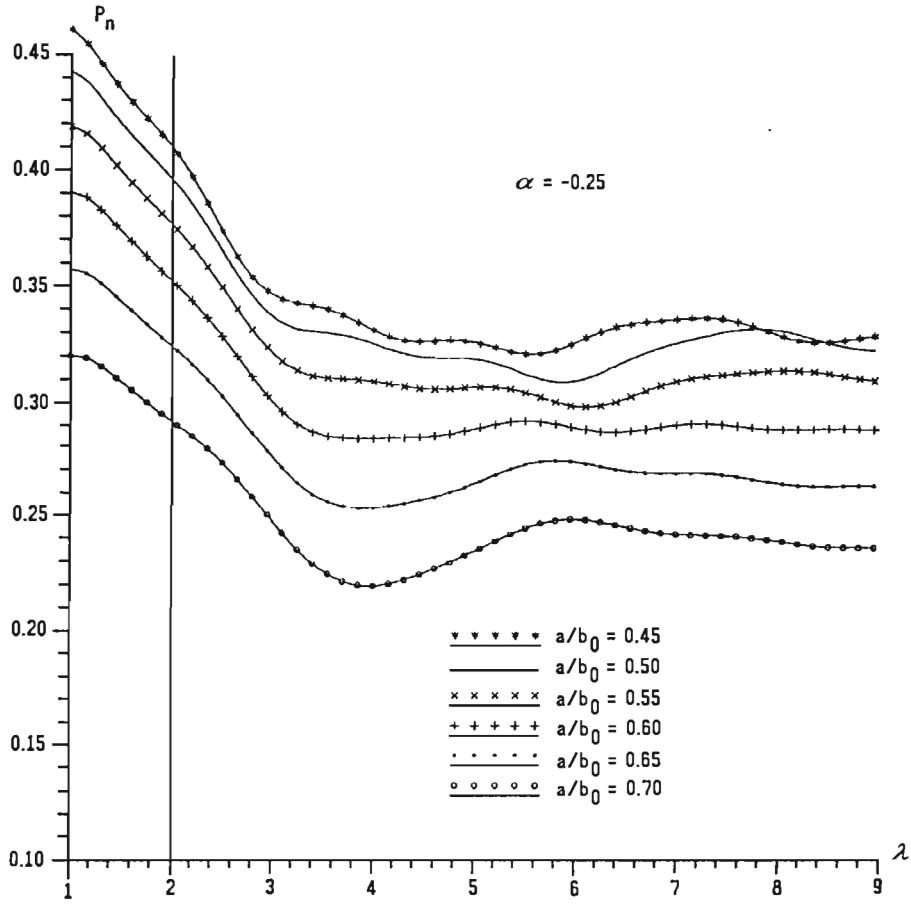

Fig. 9. Dependence of the normal reactive force on the parameter λ for $\bar{\alpha} = -0.25$

integer optimization. Total force P^* will be regarded as design objective under the constraint of constant volume.

The diagrams $P^* = f(a/b_0)$ are shown in Fig.11 for $\lambda = 2, 4, 6$ and 8; larger values of λ do not contribute to global maximum. For $\lambda = 2$ and 6 we took $\bar{\alpha} = -0.25$, and for $\lambda = 4$ and 8 we took $\bar{\alpha} = +0.25$. It is seen that $\lambda = 4$ is optimal for $a/b_0 < 0.56$, $\lambda = 6$ is optimal for $0.56 < a/b_0 < 0.66$, and $\lambda = 8$ for $a/b_0 > 0.66$. Optimal shapes are similar to those shown in Fig.6 and 8 (with slightly lower profits in the present case).

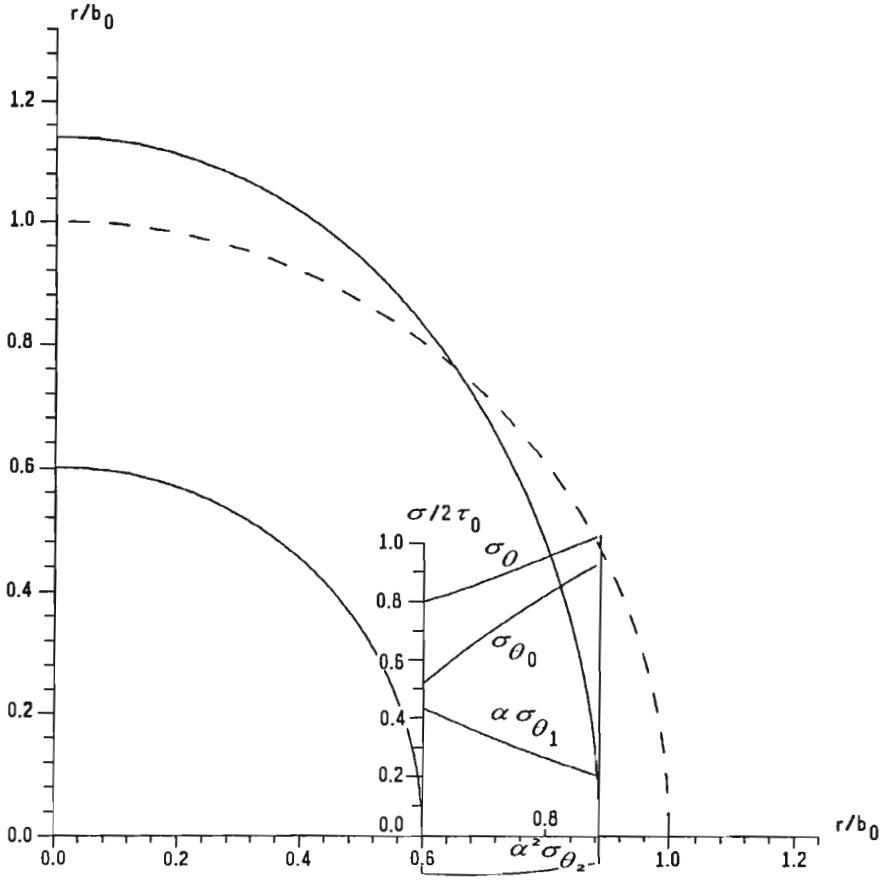

Fig. 10. Optimal shape transmitting maximal normal reactive force for $a/b_0 = 0.6$

9. Multicriterial optimization

In many engineering applications the optimization problem formulated and solved above is not adequate. Denote the external radius of the yoke for $\theta = \pi/2$ (along the "horizontal" section) briefly by B

$$B = b\left(\frac{\pi}{2}\right) = \sum_{i=0}^{\infty} b_i\left(\frac{\pi}{2}\right)\alpha^i \tag{9.1}$$

then the width of the yoke in this section equals $c = B - a$. This is an important quantity, since it should be equal to the width of the adjacent element; so, in many cases both B and a are regarded as prescribed. Such a formulation was discussed by Szczepiński and Zowczak in the above-mentioned papers, but

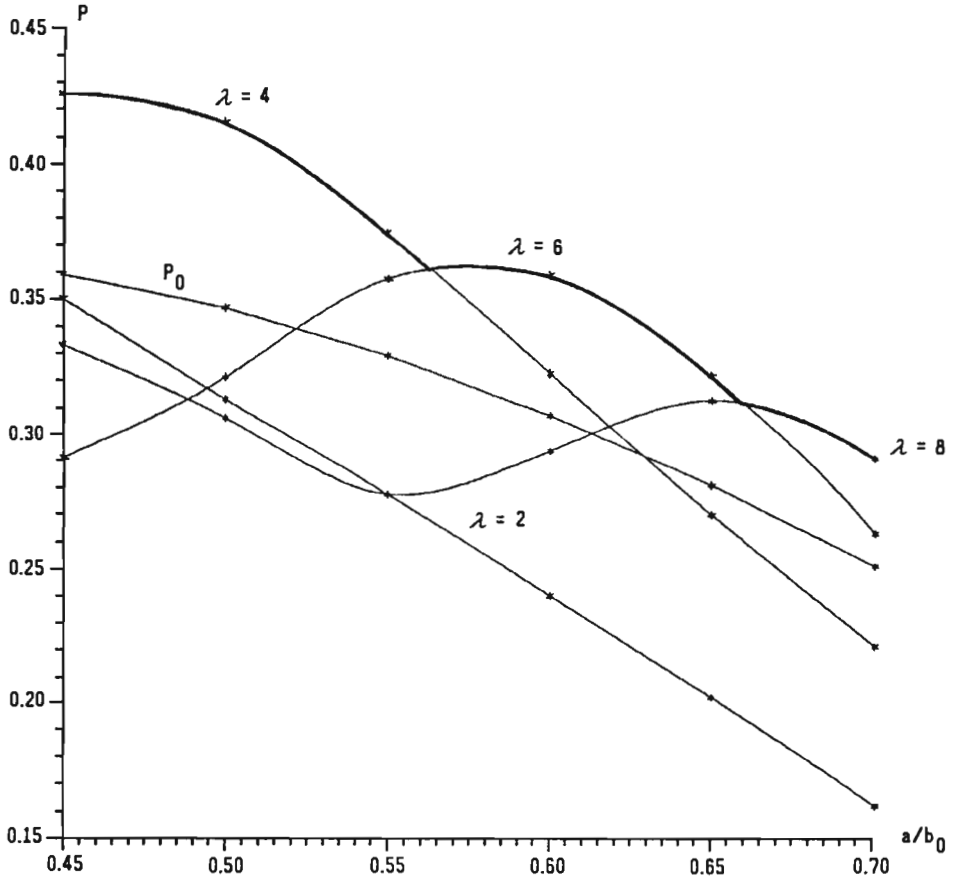

Fig. 11. Dependence of the force transmitted on the ratio a/b_0 for integer optimization

without explicit formulation of the optimization problem. This problem must now be stated as multicriterial or multiobjective optimization: we look for the optimal shape of the external contour $b(\theta)$ with two design objectives: maximization of the force transmitted and minimization of the volume of the element, under the constraints listed above (without constant volume) and an additional constraint of prescribed B.

Typical approach to multicriterial optimization consists in introduction of a preference function or substitute function thus reducing the problem to unicriterial optimization, though such a reduction is by no means unique (Osyczka, 1989). Consider, for example, minimization of all m design objectives. Usually there exists a set of solutions $\boldsymbol{x}$ minimizing in turn individual design objectives f_j, $j = 1, 2, ..., m$; denote these minimized objectives by $\bar{f}_j$. Then we form a vector

of relative losses of other solutions with respect to $\bar{f}_j$, namely

$$z_j(\boldsymbol{x}) = \frac{f_j(\boldsymbol{x}) - \bar{f}_j}{\bar{f}_j} \tag{9.2}$$

(these quantities are non-negative) and look for minimum of a certain preference function of losses $F[z_j(\boldsymbol{x})]$. From among various proposals of such functions the following linear expression seems to be sufficiently simple and general

$$F[z_j(\boldsymbol{x})] = \sum_{j=1}^{m} w_j z_j(\boldsymbol{x}) \tag{9.3}$$

where w_j are the weighting coefficients, expressing importance of individual objectives, as considered by the designer; it is convenient to assume $\sum_{j=1}^{m} w_j = 1$.

In the case of yoke elements under consideration with two design objectives, namely P to be maximized and V to be minimized, the above approach cannot be employed directly, since the optima of individual objectives P and V do not exist. One could imagine an optimum of P in the form

$$P = 2\tau_0 hc = 2\tau_0 h(B - a) \tag{9.4}$$

assuming $\sigma_\theta = 2\tau_0 = \text{const.}$, but theoretically even this value may be exceeded: looking at the yield condition (2.1) we find the possibility $\sigma_\theta > 2\tau_0$ if σ_r is positive within the interval $a < r < B$, $\theta = \pi/2$ (through σ_r is assumed to be non-positive for $r = a$ and $\sigma_r = 0$ for $r = B$). For the volume V certainly no minimum larger than zero exists if there is no constraint imposed on the force transmitted. Hence we use Eqs (9.2) and (9.3) in a suitably modified form, particularly appropriate to the perturbation method. Namely, we replace quantities (9.2) by the quantities

$$\hat{z}_j(\boldsymbol{x}) = \pm \frac{f_j(\boldsymbol{x}) - f_{j0}}{f_{j0}} \tag{9.5}$$

where f_{j0} is the value of the objective function f_j in unperturbed state; sign "+" in Eq (9.5) is used for objectives to be minimized, sign "−" for those to be maximized, then the whole problem is reduced to minimization. In contradistinction to quantities (9.2) the quantities (9.5) may be negative, moreover, they are negative as a rule. Indeed, they represent negative losses with respect to the unperturbed solution, and minimization of negative losses means maximization of positive profits. Then, in certain nonlinear preference functions F it is necessary to replace $\hat{z}_j(\boldsymbol{x})$ by $|\hat{z}_j(\boldsymbol{x})|$ with additionally introduced sign $\hat{z}_j(\boldsymbol{x})$ to keep final signs correct; in the linear expression (9.3) such a change is not necessary.

So, in the case under consideration with λ as the only design variable we introduce two relative losses

$$\hat{z}_1(\lambda) = \frac{P_0 - P(\lambda)}{P_0} \qquad \hat{z}_2(\lambda) = \frac{V(\lambda) - V_0}{V_0} \tag{9.6}$$

where P_0 and V_0 are given by Eqs (2.3) and (5.1) with b or b_0 replaced by B, and P and V are physical (dimensional) quantities. Dimensionless quantities may also be introduced for convenience, but the definitions must be changed with respect to those used before, since now b_0 is no longer constant and should be replaced by B

$$P^{**} = \frac{P}{2\tau_0 Bh} = \frac{b_0}{B} P^{*}$$
$$V^{**} = \frac{4V}{\pi B^2 h} = \left(1 - \frac{a}{b_0^2}\right) \frac{b_0^2}{B^2} . \tag{9.7}$$

Now, we make use of the solutions obtained above, but with a/b_0 adjusted in particular cases as to obtained prescribed a/B. Then we construct a preference function (9.3) for various values of weighting coefficients w_j and evaluate the optimum in each case. First we choose $a/B = 0.6$ since such a ratio was discussed in detail by Szczepiński and Zowczak. Indeed, they assumed $c/a = 2/3$, and hence $a/B = 0.6$. The results are presented in Table 1 for integer optimization, corresponding to vertical tangent at $\theta = \pi/2$, and for three configurations of weighting coefficients: F_1 is calculated for $w_1 = w_2 = 0.5$ (typical assumption), F_2 for $w_1 = 0.9$, $w_2 = 0.1$ and F_3 for $w_1 = 0.1$, $w_2 = 0.9$ (extreme assumptions). The best solutions are shown in frames. In the first variant (equal weighting coefficients) the solution for $\lambda = 6$ is the best: minimal value of weighted losses is -0.063, it means profit $+0.063$. In the second variant (with preference ascribed to the force transmitted) Zowczak's solution is the best. In the third variant (with preference ascribed to the volume) the solution for $\lambda = 8$ is the best from among the solutions considered; however, the relevant weighted loss is $+0.052$, it is positive, and hence simply the unperturbed (circular) solution is better. Other solutions given in Table 1 are not Pareto-optimal: one can always find another solution with lower values of both objective functions to be minimized.

Table 1. Multicriterial optimization for $a/B = 0.6$ and various weighting coefficients, and comparison with Szczepiński's and Zowczak's solutions

No	λ	a/b_0	P	A	z_1	z_2	F_1	F_2	F_3
1	2	0.532	0.327	0.912	-0.067	0.425	0.179	-0.018	0.376
2	4	0.571	0.371	0.744	-0.210	0.163	-0.024	-0.173	0.126
3	6	0.584	0.372	0.696	-0.214	0.088	-0.063	-0.184	0.058
4	8	0.590	0.293	0.674	0.044	0.053	0.049	0.045	0.052
5	Sz		0.4	1.123	-0.305	0.748	0.221	-0.200	0.643
6	Z		0.4	0.973	-0.305	0.520	0.108	-0.223	0.438

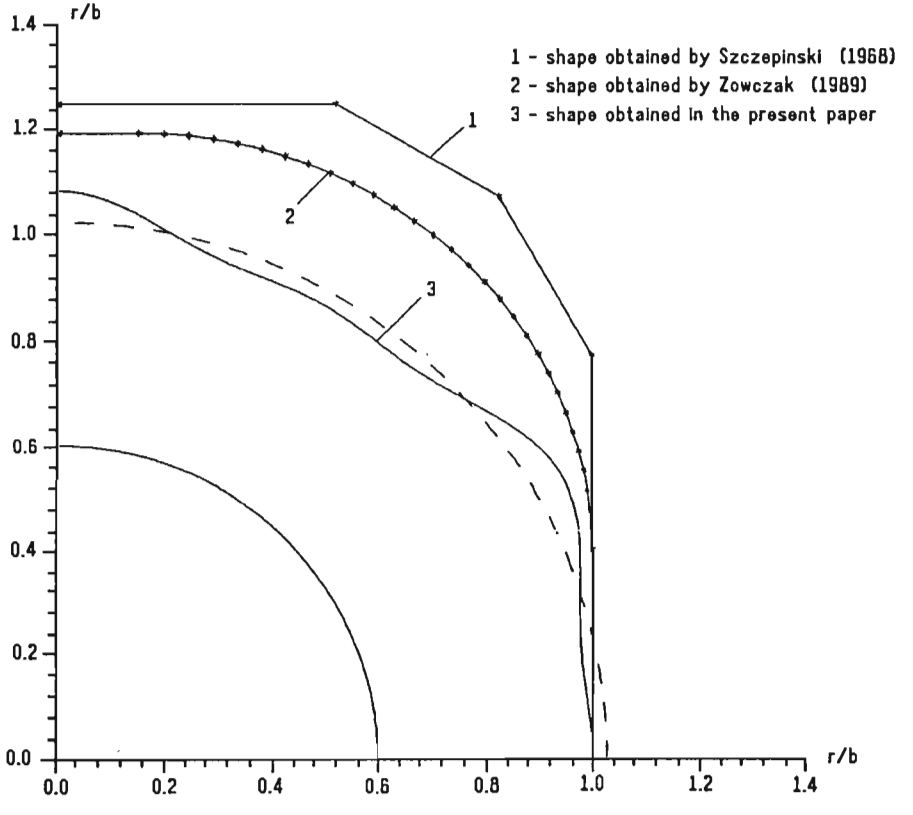

Fig. 12. Optimal shape for $a/B = 0.6$, multicriterial optimization with $w_1 = w_2 = 0.5$, $\lambda = 6$, and comparison with Szczepiński's and Zowczak's solutions

The solution for $\lambda = 6$ is shown in Fig.12 together with Szczepiński's and Zowczak's solutions. Lower value of the volume for $\lambda = 6$ is seen. The shape obtained from (5.7) is a bit wavy, but this is typical for a trigonometric series replaced by its partial sum in the form of a trigonometric polynomial. It is supposed

that subsequent terms of the series would make the shape more regular.

Table 2 brings the results for $a/B = 0.7$, and a solution obtained for this ratio by Szczepiński and Szlagowski (1990) is also quoted. In all variants the solution for $\lambda = 8$ is optimal here. Table 3 discusses the case $a/B = 0.5$, and here $\lambda = 4$ is always optimal.

Table 2. Multicriterial optimization for $a/B = 0.7$ and various weighting coefficients, and comparison with Szczepiński-Szlagowski solution

No	λ	a/b_0	P^{**}	V^{**}	z_1	z_2	F_1	F_2	F_3
1	2	0.621	0.251	0.781	-0.004	0.531	0.527	0.050	0.478
2	4	0.667	0.264	0.611	-0.056	0.198	0.142	-0.031	0.173
3	6	0.681	0.293	0.567	-0.172	0.112	-0.060	-0.144	0.084
4	8	0.689	0.304	0.542	-0.216	0.063	-0.153	-0.188	0.035
5	Sz		0.3	0.773	-0.200	0.516	0.158	-0.128	0.444

Table 3. Multicriterial optimization for $a/B = 0.5$ and various weighting coefficients

No	λ	a/b_0	P^{**}	V^{**}	z_1	z_2	F_1	F_2	F_3
1	2	0.443	0.401	1.024	-0.157	0.365	0.104	-0.105	0.313
2	4	0.476	0.446	0.853	-0.287	0.137	-0.075	-0.245	0.035
3	6	0.487	0.319	0.804	-0.080	0.072	0.076	0.079	0.073
4	8	0.492	0.318	0.783	-0.082	0.044	0.063	0.078	0.048

10. Conclusions

- The boundary perturbation method applied to yoke elements makes it possible to describe analytically a class of fully plastic solutions as a first step towards shape optimization
- Unicriterial optimization is then employed to maximize the limit load-carrying capacity under the constraint of constant volume
- If the characteristic dimensions of the yoke element are given, then both the volume and the force transmitted are subject to variations and a multicriterial optimization is necessary
- Finally, the results of the present paper are compared to those obtained earlier by Szczepiński and Zowczak. Depending on the weighting coefficients in the preference function used in multicriterial optimization, either the present solution or that given by Zowczak are regarded as optimal.

Acknowledgement
Grant KBN-1960/91 is gratefully acknowledged.

References

1. BOCHENEK B., KORDAS Z., ŻYCZKOWSKI M., 1983, *Optimal plastic design of a cross section under torsion with small bending,* J.Struct.Mech., **11**, 3, 383-400
2. DOLLAR A., KORDAS Z., 1980, *Kształty prętów silnie zakrzywionych poddanych zginaniu z rozciąganiem i ścinaniem, całkowicie uplastycznionych w stadium zniszczenia,* Mech.Teor.i Stos., **18**, 4, 603-622
3. GUZ A.N., NEMYSH YU.N., 1987, *Boundary perturbation method in continuum mechanics, a survey,* (in Russian), Prikl. Mekhanika, **23**, 9, 3-29
4. GUZ A.N., NEMYSH YU.N., 1989, *Boundary perturbation method in continuum mechanics,* (in Russian), Vyshtcha Shkola, Kiev
5. ILYUSHIN A.A., 1940, *Deformation of a viscoplastic body,* (in Russian), Uchebn. Zapiski Mosk. Gosud. Univers., **39**
6. IVLEV D.D., 1957, *Approximate solutions to elastic-plastic problems of perfect plasticity,* (in Russian), Dokl. AN SSSR, **113**, 2
7. KORDAS Z., 1977, *Problematyka określania kształtów ciał wykazujących całkowite uplastycznienie w stadium zniszczenia,* Zesz. Nauk. Pol. Krak., Podst. Nauki Techn., **7**
8. KORDAS Z., 1979, *Determination of noncircular shapes of doubly-connected disks showing full yielding at collapse,* Bull. Acad.Pol.Sci., Ser. Sci. Techn., **27**, 7, 279-286
9. KORDAS Z., POSTRACH H., 1990, *Niekolowe kształty dwuspójnych tarcz wirujących, całkowicie uplastycznionych w stadium zniszczenia,* Prace Komisji Mech. Stos. Oddz. Krak. PAN, **14**, 25-36
10. KORDAS Z., SKRABA W., 1977, *Design of thick-walled cylinders subject to internal pressure and bending under the condition of full plasticization at the stage of collapse,* Bull. Acad.Pol.Sci., Ser. Sci. Techn., **25**, 4, 119-129
11. KORDAS Z., ŻYCZKOWSKI M., 1970, *Investigation of the shape of non-circular thick-walled cylinders subject to full yielding at the stage of plastic collapse,* Bull. Acad.Pol.Sci., Ser. Sci. Techn., **18**, 10, 839-847
12. MORSE P.M., FESHBACH H., 1953, *Methods of theoretical physics,* Vol 2, McGraw-Hill, New York
13. OSYCZKA A., 1989, *Computer aided multicriterion optimization system (CAMOS),* Proc. GAMM Seminar "Discretization Methods and Structural Optimization", Siegen 1988, Springer, 263-270
14. PARNES R., 1987, *The boundary perturbation method in elastostatics: investigation of higher order effects and accuracy of solutions,* J. Méc. Théor. Appliquée, **6**, 2, 295-314
15. PARNES R., 1989, *Bending of simply-supported elliptic plates: BPM solutions with second-order derivative boundary conditions,* J. Appl. Mech., **56**, 21, 356-363

16. SCHNACK E., IANCU G., 1989, *Shape design of elastostatic structures based on local perturbation analysis,* Struct. Optimization, **1**, 2, 117-126

17. SPENCER A.J.M., 1962, *Perturbation methods in plasticity, II, plane strain of slightly irregular bodies,* J. Mech. Phys. Solids, **10**, 1, 17-26

18. SZCZEPIŃSKI W., 1966, *Optimum design of plane elements with complex shape,* Arch. Mech. Stos., **18**, 2, 193-211

19. SZCZEPIŃSKI W., 1968, *Projektowanie elementów maszyn metodą nośności granicznej,* PWN Warszawa

20. SZCZEPIŃSKI W., SZLAGOWSKI J., 1990, *Plastic design of complex shape structures,* PWN-Horwood, Warszawa-Chichester

21. ZOWCZAK W., 1981, *Projektowanie i nośność graniczna elementów połączeń sworzniowych,* Rozpr. Inż., **29**, 2, 267-278

22. ZOWCZAK W., 1981, *Projektowanie elementów konstrukcyjnych przy pomocy ciągłych pól statycznie dopuszczalnych,* Mech.Teor.i Stos., **19**, 4, 563-573

23. ZOWCZAK W., 1989, *O wymiarowaniu elementów jarzmowych metodą charakterystyk,* Rozpr. Inż., **37**, 3, 565-574

24. ŻYCZKOWSKI M., 1981, *Combined loadings in the theory of plasticity,* PWN-Nijhoff, Warszawa-Aalphen

W sprawie optymalnego kształtowania plastycznego elementów jarzmowych

Streszczenie

Praca poświęcona jest optymalnemu kształtowaniu elementów jarzmowych (jarzma, łby korbowodów, ogniwa łańcuchów itp.) pod założeniem idealnej plastyczności materiału. Kształtowanie przebiega w dwóch etapach: w pierwszym, korzystając z metody zakłócenia konturu, określa się klasę rozwiązań wykazujących całkowite uplastycznienie w stadium zniszczenia, natomiast w drugim dokonuje się optymalizacji w tej klasie. Zastosowano jednokryterialną optymalizację w przypadku doboru największej nośności granicznej dla elementów o stałej objętości. Jeżeli jednak dane są charakterystyczne wymiary jarzma, to wówczas niezbędna jest optymalizacja wielokryterialna. Dokonano również porównania z rozwiązaniami uzyskanymi wcześniej przez innych autorów.

Manuscript received January 25, 1993; accepted for print May 17, 1993